A Freeze-Fracture Transmission Electron Microscopy and Small Angle X-Ray Diffraction Study of the Effects of Albumin, Serum, and Polymers on Clinical Lung Surfactant Microstructure

Andreas Braun,* Patrick C. Stenger,* Heidi E. Warriner,* Joseph A. Zasadzinski,* Karen W. Lu,[†‡] and H. William Taeusch[†‡]

*Department of Chemical Engineering, University of California, Santa Barbara, California 93106; [†]Department of Pediatrics, University of California, San Francisco; and [‡]San Francisco General Hospital, San Francisco, California 94110

ABSTRACT   Freeze-fracture transmission electron microscopy shows significant differences in the bilayer organization and fraction of water within the bilayer aggregates of clinical lung surfactants, which increases from Survanta to Curosurf to Infasurf. Albumin and serum inactivate all three clinical surfactants in vitro; addition of the nonionic polymers polyethylene glycol, dextran, or hyaluronic acid also reduces inactivation in all three. Freeze-fracture transmission electron microscopy shows that polyethylene glycol, hyaluronic acid, and albumin do not adsorb to the surfactant aggregates, nor do these macromolecules penetrate the interior water compartments of the surfactant aggregates. This results in an osmotic pressure difference that dehydrates the bilayer aggregates, causing a decrease in the bilayer spacing as shown by small angle x-ray scattering and an increase in the ordering of the bilayers as shown by freeze-fracture electron microscopy. Small angle x-ray diffraction shows that the relationship between the bilayer spacing and the imposed osmotic pressure for Curosurf is a screened electrostatic interaction with a Debye length consistent with the ionic strength of the solution. The variation in surface tension due to surfactant adsorption measured by the pulsating bubble method shows that the extent of surfactant aggregate reorganization does not correlate with the maximum or minimum surface tension achieved with or without serum in the subphase. Albumin, polymers, and their mixtures alter the surfactant aggregate microstructure in the same manner; hence, neither inhibition reversal due to added polymer nor inactivation due to albumin is caused by alterations in surfactant microstructure.

INTRODUCTION

Lung surfactant is a mixture of lipids (primarily dipalmitoylphosphatidylcholine (DPPC)) and four lung surfactant specific proteins (SP-A, -B, -C, and -D) that lines the interior of the lung alveoli and acts to lower the interfacial tension in the lungs, thereby insuring a negligible work of breathing and uniform lung inflation (1,2). The absence of lung surfactant due to prematurity leads to neonatal respiratory distress syndrome (NRDS) (1,3–5). Treating NRDS with currently available replacement surfactants has significantly reduced neonatal mortality in developed countries (1,3–5). However, replacement surfactant treatment has been disappointing when used to treat lung diseases associated with lung injury and acute respiratory distress syndrome (ARDS) (6–8). In such cases, surfactant loses the ability to reduce surface tension and is said to be ''inactivated'' (4,9–11). Surfactant inactivation caused by serum leakage into alveoli is one reason treatment of lung injuries with surfactant has been unsuccessful (12,13). Several nonionic and anionic polymers have recently been shown to enhance the ability of clinical surfactants to resist inactivation by serum and other substances (9,14–21). Lung function of animals with lung injury is markedly improved when polymers are added to clinical surfactants used for treatment of NRDS (9,11,16,22–24).

Surfactant inactivation is also a likely factor in the development and progression of ARDS. ARDS has an incidence of 150,000 cases per year (U.S.) and a mortality rate of ~30% (4,8,25). The pathophysiology of ARDS involves injury to the alveolar-capillary barrier, lung inflammation, atelectasis, surfactant dysfunction, and intrapulmonary shunting. No specific therapy for ARDS currently exists. Although ARDS has a more complicated pathology than the simple absence of surfactant, ARDS shares many NRDS features such as diminished lung compliance, marked restriction of lung volumes, and profound hypoxemia. Hence, it was hoped ARDS might respond favorably to surfactant replacement therapy. However, clinical trials with the most effective formulations used in NRDS yield gains in ARDS patients that are both modest and transient (4,6,7,25–28), suggesting that ARDS involves not only a lack of functional surfactant, but also an inactivation of the endogenous or exogenous surfactant present.

In ARDS, increased concentrations of serum proteins in the alveolar hypophase are a likely cause of inactivation; albumin concentrations in ARDS alveolar fluid may reach 100 mg/ml, with an average concentration reported by Ishizaka and co-workers of 25 mg/ml (29). Albumin and other serum proteins are surface active and can quickly adsorb to the alveolar air-water interface to form a barrier to surfactant adsorption (17,18,30). A common finding is that increased

concentrations of surfactant and increased fractions of surfactant-specific proteins SP-A and SP-B reduce inactivation (12,31–38). A more surprising finding is that hydrophilic, nonadsorbing, nonionic, and anionic polymers added to aqueous mixtures of clinical surfactants (which contain SP-B and SP-C, but not SP-A) reduce inactivation by serum, meconium, albumin, and other substances both in vitro and in vivo (9–11,14,16,22,39–41).

How polymers reverse surfactant inactivation is an open question. Previous researchers have speculated that there is a relationship between inhibition and surfactant microstructure (42–44) based on transmission electron microscopy of chemically fixed clinical lung surfactants. However, clinical surfactants are >98% lipid (see Table 1), and lipid aggregates are notoriously difficult to fix via conventional glutaraldehyde/osmium tetroxide fixation and dehydration methods (45–48). No chemical fixative reacts significantly with saturatured lipids such as DPPC (45), which is the dominant lipid in lung surfactant. Hence, a significant fraction of the lipid is lost by extraction during specimen preparation, and all information about the distribution of water in the sample is lost (43). In comparison, rapid freezing methods (49) followed by freeze-fracture replication can provide artifact-free images of lipid bilayer samples in their hydrated state with no added chemical fixatives, while preserving both the distribution of the aggregates in the original dispersion and the microstructure and bilayer organization of the aggregates (49–56).

Freeze-fracture transmission electron microscopy (FFTEM) (49,50,52,54–63) of the clinical lung surfactants Survanta, Curosurf, and Infasurf was used to determine the size and shape distribution of the surfactant aggregates in the suspension and the organization of the bilayers within the aggregates before and after exposure to albumin and polymers. Survanta, Curosurf, and Infasurf are clinical replacement lung surfactants in widespread use in the U.S. and Europe to treat NRDS. Although they differ in composition of both lipid and protein constituents, the effects of these differences are not clear. All are effective in clinical trials, and comparison trials do not conclusively show advantages of one over the other (64,65). Survanta is made from minced bovine lung extract with the addition of DPPC, palmitic acid, and triacylglycerol. Curosurf is an extract of whole mince of porcine lung tissue purified by column chromatography. Infasurf is a chloroform-methanol extract of neonatal calf lung lavage. These three surfactants are primarily lipid (>98%) but contain small fractions of the surfactant proteins SP-B and SP-C (but not SP-A and SP-D) (66). The compositions of the three surfactants are compared in Table 1.

FFTEM shows significant differences in the bilayer organization of the clinical lung surfactants. The major difference is the fraction of water within the bilayer aggregates, which increases from Survanta to Curosurf to Infasurf. Although each clinical surfactant has its own distinct bilayer organization, freeze-fracture images show that albumin and polymers do not adsorb to any of the clinical surfactant aggregates. Rather, both albumin and polymers act to dehydrate the surfactant aggregates by creating an osmotic pressure difference between the interior of the aggregate and the exterior. The aggregates expel any interior pockets of water and the bilayer order is increased. There is clear evidence of fusion of smaller aggregates to form larger aggregates, in addition to the flocculation observed via optical microscopy. Small angle x-ray scattering shows that the d-spacing of Curosurf, Survanta, and Infasurf depends on the polymer and/or albumin concentration, consistent with the polymer and albumin not being able to access the interior of the aggregates (67). The exponential dependence of the d-spacing of Curosurf on the osmotic pressure shows that the repulsive forces between the bilayers are due to electrostatic double-layer forces, with a characteristic decay length determined by the ionic strength of the solution (67–69).

Albumin, polymers, and their mixtures alter the surfactant aggregate microstructure in the same manner; this implies that albumin does not inactivate surfactant by alterations in surfactant microstructure. In addition, the microstructure alterations of polyethylene glycol (PEG) and other polymers do not themselves reverse surfactant inactivation. This has been shown by comparing the effects of 5 wt % 10 kDa PEG with 0.25 wt % 250 kDa hyaluronic acid (HA) on surfactant microstructure and surfactant inactivation. Pulsating bubble surfactometer (PBS) measurements show that these polymer concentrations are sufficient to reverse inactivation of Survanta, Curosurf, and Infasurf; the lower HA concentration actually provides more complete inactivation reversal than does the

TABLE 1 Consensus lipid composition (%, g/g of total lipid) and protein concentration (% phospholipid, g/g) of clinical surfactants

	Native Surfactant	Curosurf	Infasurf	Survanta
PC % (w/w)	70–85	67–74	70–74	79–87
DPPC (%PC)	36–59	50–56	41–61	45–75
LPC	0.5	<1		1
Sphingomyelin	2	8.1	2	4.8
Cholesterol	5	0	5	0
PI	4–7	3.3	~2	0.5
PS	5		~2	
PE	3	4.5	3	2.2
PG	7–10	1.2	6	3.2
PA				6–14
Unknown			4.3	
SP-A	4	0	0	0
SP-B	1	0.3	0.4–0.9	0.04–0.13
SP-C	1	0.7	0.6	0.9–1.65
SP-D	4	0	0	0

PC, phosphatidylcholine; DPPC, dipalmitoylphosphatidylcholine; LPC, lysophosphatidyl choline; PI, phosphatidylinositol; PS, phosphatidylserine; PE, phosphatidylethanolamine; PG, phosphatidylglycerol. Range of reported averages are taken from the following sources: (Curosurf, Package inserts from Chiesi Farmaceutici, Parma, Italy; ONY, New York; and Survanta, Ross Labs, Ohio) (33,64,66,104,105).

higher PEG concentration. As osmotic pressure, Π_{os}, is proportional to the number of polymers in a dilute solution, $\Pi_{os} \approx (w_p/M)\,RT$, ($\Pi_{os}$ in dynes/cm^2, w_p is the weight fraction polymer, M is the molar mass in g/mole, R is the gas constant, 8.314×10^7 g-cm^2/(s^2-mole-K), and T is the absolute temperature (67)), the PEG solution has an osmotic pressure more than 100 times higher than the HA solution. FFTEM shows that PEG significantly alters the bilayer organization of the surfactant aggregates, whereas HA does not. In addition, FFTEM images show that Survanta aggregates are changed minimally, whereas Infasurf and Curosurf undergo extensive rearrangements with 5 wt % PEG; however, all three surfactants show inactivation reversal with 5 wt % PEG. Hence, inactivation reversal does not correlate with the extent of surfactant aggregate disruption caused by polymers.

MATERIALS AND METHODS

Infasurf (Forest Pharmaceuticals, St. Louis, MO) was purchased from the hospital pharmacy at University of California, San Francisco. Survanta (Abbott Laboratories, Columbus, OH) was obtained from the San Francisco General Hospital nursery. Curosurf was purchased from Dey Laboratories (Napa, CA). Curosurf, Infasurf, and Survanta are suspensions of bilayer aggregates in 0.15 M NaCl at total concentrations of 80, 35, and 25 mg/ml, respectively, and are refrigerated for storage. Before use, the surfactant suspensions are equilibrated at room temperature and swirled gently to obtain a homogeneous suspension. The suspensions are diluted as needed with freshly prepared saline buffer (150 mM NaCl (EM Science; Gibbstown, NJ), 2 mM CaCl$_2$ (Acros Organics, Geel, Belgium; Fisher Scientific, Pittsburgh, PA), and 0.2 mM NaHCO$_3$ (EM Science) in deionized water and adjusted to pH = 7.0) to the desired concentration. The consensus compositions of the clinical surfactants and human lung surfactant are given in Table 1.

Polyethylene glycol (PEG; 10 kDa) and bovine serum albumin were purchased from Sigma (St. Louis, MO). HA (250 kDa) was a gift from GlycoMed Research, (New York, NY). Samples containing polymer and/or albumin were prepared by mixing stock solutions of polymer and/or albumin with concentrated surfactant suspensions, then diluting with saline buffer to the desired concentration. The samples are swirled gently and equilibrated overnight in the refrigerator. Samples are allowed to equilibrate at room temperature before use.

Native surfactant was obtained by saline bronchoalveolar lavage of calf lung. The recovered lavage fluid was centrifuged at $500 \times g$ for 10 min followed by further centrifugation in distilled water at $17,000 \times g$ for 2 h at 10°C. The pellet obtained was lyophilized and stored at 4°C before use. The concentration of native calf surfactant was determined by lipid phosphorus after Bligh-Dyer extraction (70). Serum was obtained from normal adult laboratory volunteers and also kept frozen at −80°C. Protein content of sera was 6.8 g/dl.

Surface activity measurement

Native surfactant was resuspended in 0.9% NaCl at a concentration of 1.0 mg/ml. The therapeutic surfactants were diluted with 0.9% saline to 1.25 mg/ml. Dry polymers (PEG, HA, or dextran) were added to surfactants and mixed by vortex for ~60 s at room temperature to a final concentration of 5% (w/v) (PEG and dextran) or 0.25% (HA). Samples were mixed again by vortex before testing. Serum was used as a nonspecific inhibitor of surfactant in these experiments. Five microliters of serum/ml of surfactant suspension were used for inactivation of Curosurf and Infasurf. A total of 10 μl/ml of serum was used to inactivate Survanta and native surfactant. These serum concentrations relative to surfactants were selected by requiring the minimum surface tension to be above 14 mN/m after cycling for 5 min in the absence of polymer.

Surface activities were measured in a modified PBS (Electronetics, Buffalo, NY), using a technique to prevent the wetting of the capillary tube (71). Twenty seconds after formation of an initial static bubble, the microbubble was inflated and deflated at 20 cycles per min with a radius varying between 0.4 mm and 0.55 mm. The temperature of the sample chamber was maintained at 37°C. Minimum and maximum surface tensions were recorded at the 10th cycle (after 30 s of cycling) and after 5 min. The surface tension was calculated by the Laplace equation, $P = 2\gamma/r$, where γ is the surface tension, P the inflating pressure, and r the bubble radius. We defined ΔA_{10} as the change in bubble size necessary for surface tension to fall to 10 mN/m. That is, $\Delta A_{10} = $ [(maximum surface area (SA) − SA @10 mN/m)/maximum SA] $\times$ 100. If the surface tension did not reach 10 mN/m, then we assigned a value of 47% for ΔA_{10}, that being the maximum difference in surface area between the largest and smallest bubble during cycling. The data are presented as means $\pm$ SE. Group differences were analyzed by one way analysis of variance (ANOVA). Tukey or Kruskal-Wallis tests were used to correct for multiple comparisons and a corrected $p < 0.05$ was considered significant.

Small angle x-ray diffraction

Small angle x-ray scattering experiments were performed on a custom-built instrument with an 18-kW Rigaku rotating anode source (CuK$_\alpha$, $\lambda = 1.54$ Å, Rigaku, The Woodlands, TX) and 2-d area detector. The instrument is optimized for very small angle work (5–60 nm) and has an Osmic Confocal Maxflux double focusing multilayer mirror (Osmic, Auburn Hills, MI), an 11-cm Bruker HI-STAR multiwire area detector (Bruker, Billerica, MA), and a 1.5-m sample to detector distance. The full width at half-maximum was $<\sim 0.005$ Å^{-1}. In all experiments, samples were loaded into 1.5-mm borosilicate glass capillaries (Charles Supper, Natick, MA) and flame sealed. Temperature control was via circulating heated or cooled fluid through an aluminum sample holder block, monitored by a thermistor located adjacent to the capillary (72).

Freeze-fracture electron microscopy

Freeze-fracture samples were prepared by first depositing a film of sample liquid ~100 microns thick between two copper planchettes. The samples were frozen by plunging the sample into a liquid propane/liquid ethane bath cooled by liquid nitrogen. The frozen sample was transferred under liquid nitrogen to the sample block of an RFD-9010 (RMC, Tucson, AZ, discontinued) freeze-fracture device. After temperature (−170°C) and pressure ($<10^{-7}$ torr) equilibration, the sample was fractured and the two resulting surfaces were replicated with ~1.5 nm platinum deposited at a 45° angle, followed by ~15 nm of carbon deposited normal to the surface. The copper planchettes were dissolved in chromerge (a mixture of chromic acid, sulfuric acid, and water), and then the replicas were washed in water and allowed to stand in ethanol several days to dissolve any remaining surfactant. The replicas were collected on formvar-coated TEM grids (Ted Pella, Redding, CA) (49). A Gatan charge-coupled device camera (Gatan, Pleasanton, CA) was used to record digital brightfield images using an FEI Technai (Eindhoven, Netherlands) transmission electron microscope at 100 KeV.

RESULTS AND DISCUSSION

As received, the Curosurf suspension consisted of multilamellar aggregates with a broad size distribution ranging from 100 nm to 3 μm (Fig. 1, A and B). The larger aggregates were invariably multilamellar but with poorly organized bilayer arrangements with ''pockets'' of water within the
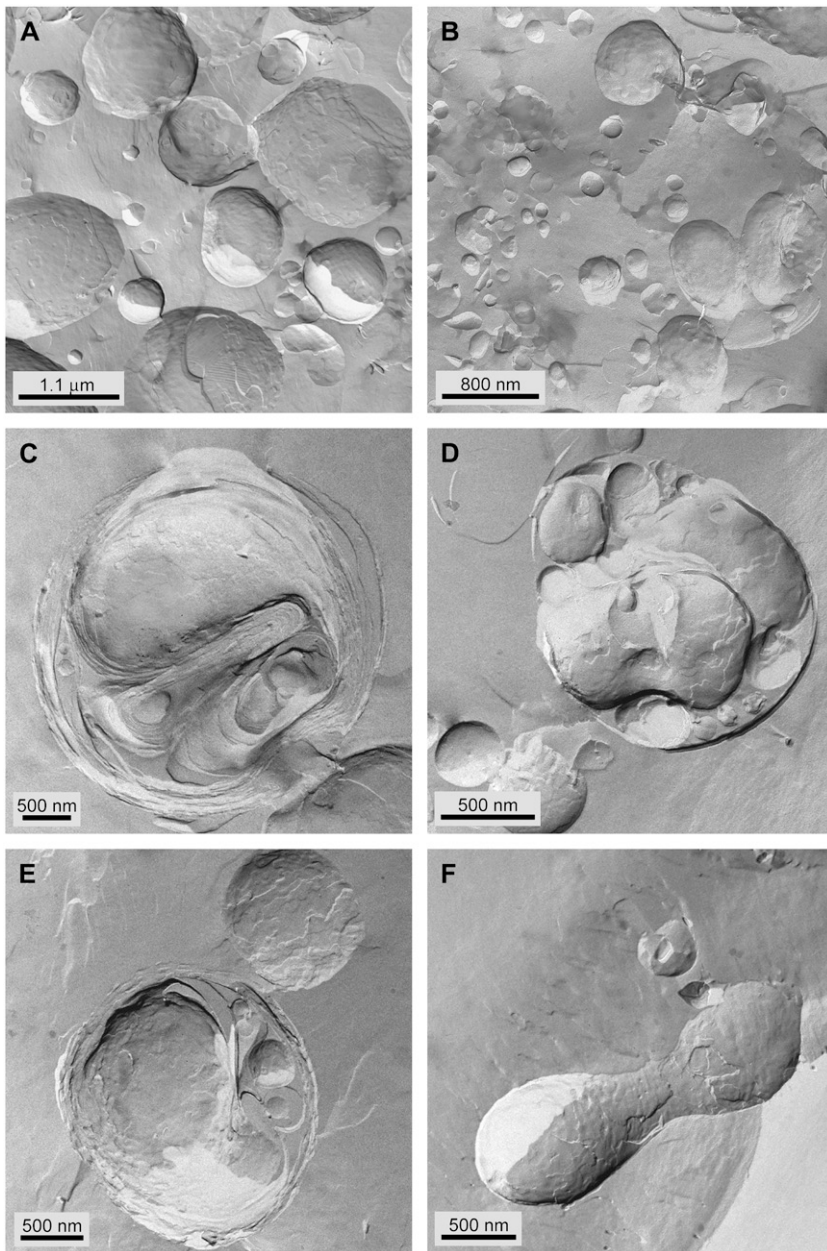
FIGURE 1 FFTEM images of Curosurf at a concentration of 80 mg/ml (*A, B*) and 10 mg/ml (*C–F*), quenched from room temperature. (*A, B*) Multilamellar aggregates with a broad size distribution. The smallest spherical particles may be unilamellar vesicles. (*C–E*) Multilamellar aggregates often had some void space between bilayers and ''pockets'' of water within the aggregate. This is consistent with the small angle x-ray scattering that showed broad reflections indicative of poor correlations between the bilayers. (*F*) Multilamellar dumbbell-shaped aggregate.

aggregate. The bilayers within the aggregates were not well correlated, consistent with the small angle x-ray diffraction showing broad reflections at these conditions (see Fig. 10 *A*). Diluting the suspension to 10 mg/ml with saline buffer (Fig. 1, *C–F*) did not change the appearance of the aggregates or the d-spacing. The aggregate shapes varied from spheroidal to dumbbell shaped (Fig. 1, *E* and *F*). The interior of the aggregates were not as well organized as typical phosphatidylcholine aggregates in water (46,50). No changes were observed when any of the clinical surfactants was diluted with saline buffer, consistent with the general behavior and microstructure of multilamellar liposomes (46,50,63).

Infasurf showed distinctly different structures than Curosurf. Infasurf consists of relatively monodisperse, unilamellar ves-

icles of diameter 250 nm $\pm$ 100 nm (Fig. 2 *A*), a substantial fraction of which are trapped within one or more bilayers to form particles ranging from 0.5 to 4 μm (Fig. 2, *B–F*). There is a significant amount of water within each aggregate, distributed throughout the void spaces between and within the small vesicles inside each larger aggregate. Structurally, the Infasurf particles are similar to ''vesosomes'', a drug delivery vehicle made by entrapping small vesicles within a larger vesicle (54,73,74). Previous work on vesosomes has shown that cholesterol can lead to this type of vesicle within vesicle structure (73,74); Infasurf is the only clinical surfactant with a significant fraction of cholesterol (Table 1).

Survanta had the largest aggregates, which consisted of well-organized stacks of bilayer sheets (Fig. 3, *A–C*) that
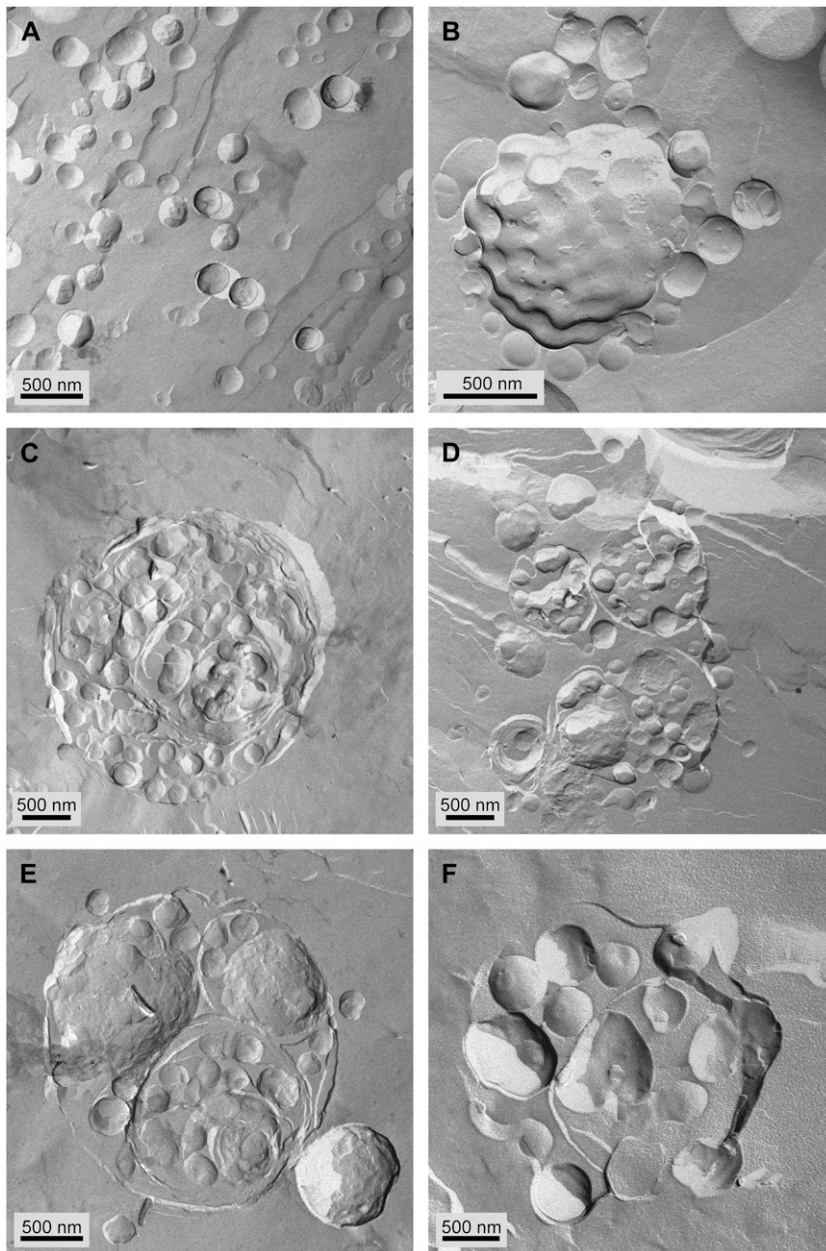
FIGURE 2   FFTEM images of Infasurf at a concentration of 10 mg/ml, quenched from room temperature. (*A*) Small, fairly monodisperse unilamellar vesicles with average diameter of 250 nm $\pm$ 100 nm. (*B*) Densely packed small vesicles within another bilayer membrane, indicated by the bumpy surface, where the densely packed vesicles push against the outer membrane. Small vesicles appear to be loosely bound to the larger aggregate. (*C–F*) Cross-fractured Infasurf aggregates with densely packed interior vesicles and large water pockets. The diameters range from 0.5 to 4 μm. The structures are similar to vesosomes, a vesicle in vesicle drug delivery vehicle (73,74).

extended over microns. Individual aggregates were too large to obtain an accurate size from FFTEM (See optical images in Fig. 4). In addition to the large bilayer aggregates, a few small unilamellar vesicles of 50–300 nm were found (Fig. 3, *B* and *D*). These aggregates were similar to pure DPPC aggregates in microstructure (62,75,76); Survanta has the highest concentration of DPPC of any of the clinical surfactants (Table 1). No water pockets or voids were observed within the aggregates, as with Curosurf and Infasurf.

Optical phase contrast microscopy of the diluted Survanta suspension showed aggregate sizes ranging from 5 to 60 μm. There were a variety of aggregate shapes, from large open bilayer fragments (Fig. 4 *A*, *arrow*), loosely packed bilayer aggregates (Fig. 4, *B–D*), and more tightly packed multilayer aggregates (Fig. 4, *B* and *C*).

Albumin effects on surfactant microstructure

Serum is known to inactivate lung surfactants in vitro, and serum protein levels are elevated in ARDS patients (12,13,29,31). Albumin is the most common surface active protein in serum (77) and was used in the freeze-fracture and small angle x-ray experiments to quantify the protein concentration and osmotic pressure. Albumin and many other serum proteins found in the bronchial fluid of ARDS patients are surface active and have a surface tension that is a
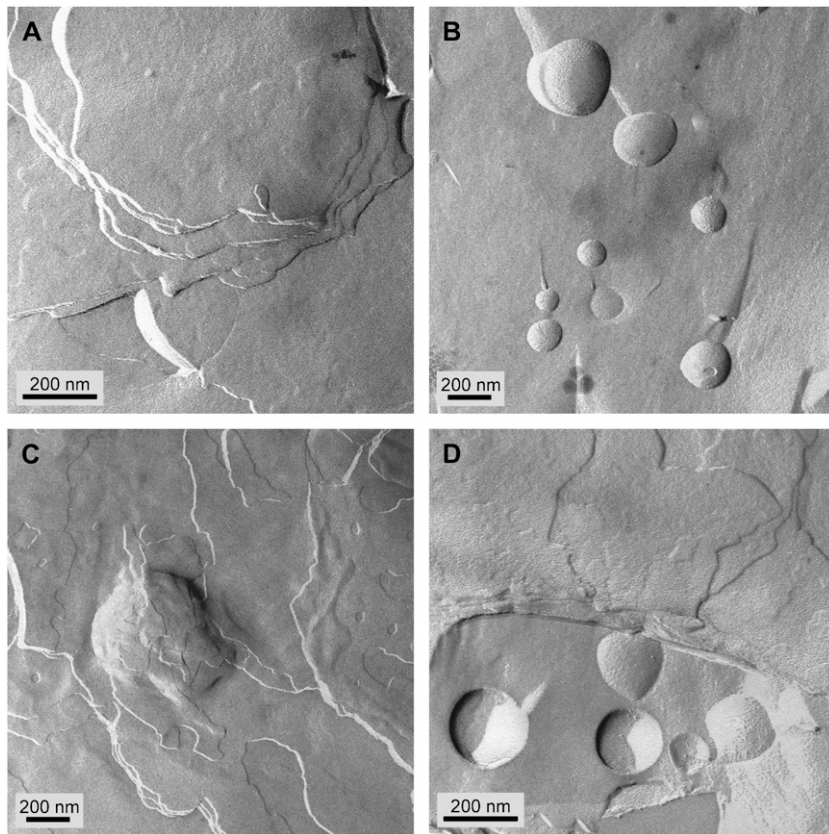
FIGURE 3 FFTEM images of Survanta at a concentration of 10 mg/ml (*A*, *B*) and 2 mg/ml (*C*, *D*), quenched from room temperature. (*A*, *C*) Most aggregates were too large to be imaged as individual particles in TEM. Here we shod the multilamellar stacks of well-ordered bilayers within the larger aggregates. There are no water pockets within the Survanta particles. (*B*, *D*) The only other structures observed are small vesicles that range from 50 to 300 nm in diameter.

logarithmic function of protein concentration up to a saturation concentration, which is ~1 mg/ml for albumin (30,77). Because of its modest molecular weight, albumin is easily leaked into airspaces during lung injury when endothelial and epithelial damage occurs. Albumin concentrations in ARDS alveolar fluid may reach 100 mg/ml, with an average concentration reported by Ishizaka and co-workers of 25 mg/ml (29). An added benefit for these experiments on rapid surfactant inactivation is that albumin has little chemical reactivity with surfactant, unlike other inflammatory proteins (e.g., phospholipases) that make in vitro experiments at times difficult to interpret. The measured minimum surface tension, γ_{min}, for human serum and many of the proteins present in serum, such as albumin, hemoglobin, thrombin, IgG, and IgM, is within a rather narrow range of 45–50 mN/m (77), independent of the details of the protein structure, molecular weight, or function (77). In vitro, albumin concentrations greater than the saturation concentration of 1 mg/ml inactivate lung surfactant (30,78).

However, Fig. 5 shows that albumin concentrations 0.5–5 mg/ml have little effect on the microstructure of Curosurf. Albumin does not appear to adsorb or interact significantly with the Curosurf aggregates over the range of concentration that inactivates surfactant. Individual albumin molecules adsorbed to the interface would appear as distinct 5–10-nm-high bumps or pits on the bilayer surfaces. This is consistent with

the small angle x-ray scattering that shows that the primary effect of albumin is as an osmotic agent that cannot penetrate the bilayers of the aggregate (see Fig. 9). Fig. 6 shows that Infasurf and Survanta also are not altered in 2 mg/ml albumin. The osmotic pressure of a 2 mg/ml albumin solution is ~10^3 dynes/cm^2, which is not sufficient to alter the spacing of the bilayers (see Fig. 9). Although Infasurf, Curosurf, and Survanta have quite different compositions and microstructures, albumin does not adsorb to or alter the lamellar organization of any of the clinical surfactants at concentrations at which surfactant is inactivated.

Hydrophilic, nonadsorbing polymers added to aqueous mixtures of clinical surfactants (which contain SP-B and SP-C, but not SP-A) reduce rapid inactivation in vitro and in vivo (Table 2). Animal studies have shown that these polymers can reverse clinical surfactant inactivation (9–11,14,16,22,39–41). Fig. 7 (18) shows the dramatic effects of 5 wt % 10 kDa PEG on the dispersions of clinical surfactants. The added polymer leads to a rapid flocculation of each of the surfactant dispersions. The flocculation is reversible; gentle agitation can break up the flocs, which can then reform over the course of minutes. This is typical for any dispersion when a nonadsorbing polymer is added (18,79).

Freeze-fracture TEM images of individual Curosurf aggregates showed significant differences with the addition of PEG (Fig. 8). Although there was little change in the average
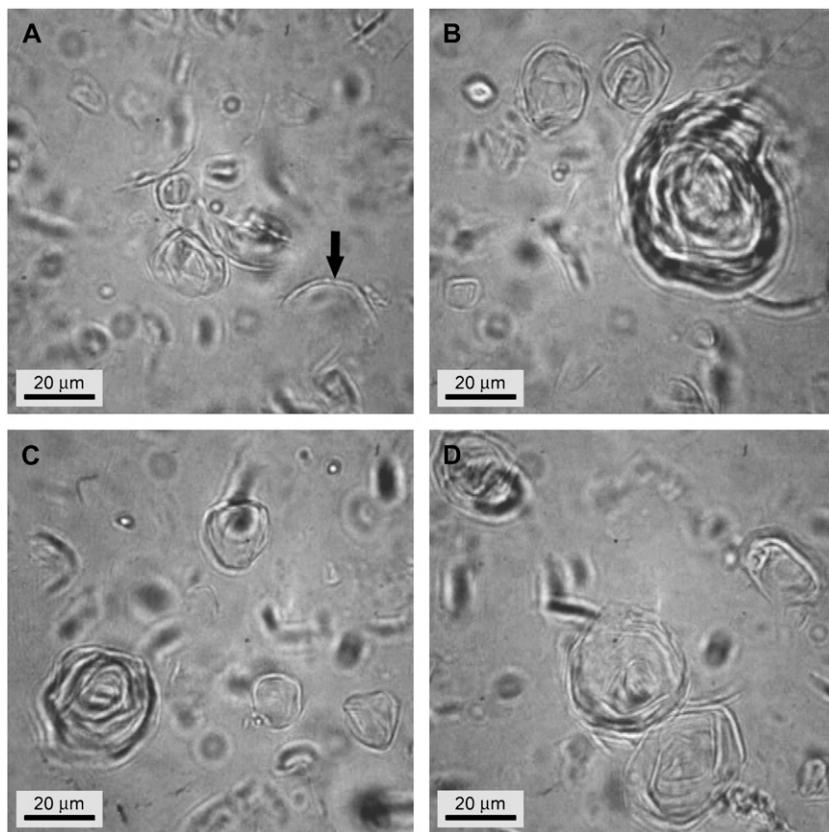
FIGURE 4 Optical phase contrast microscopy images of Survanta at a concentration of 1 mg/ml. Aggregates size range from 5 up to 60 μm and show large open bilayer structures (*A*, *arrow*), low density bilayer aggregates (*B*, *D*), and higher density multilayer aggregates (*B*, *C*).

aggregate size, the organization of the bilayers within the aggregates was altered: the average bilayer spacing decreased and there were no longer any void spaces within the aggregates. The bilayers are much better organized after exposure to PEG (see Figs. 9 and 10).

Small angle x-ray scattering confirmed that the added polymer acted to dehydrate the aggregates and decrease the d-spacing between the bilayers (Fig. 9). Consistent with earlier results (67), macromolecules such as 10 kDa PEG or albumin cannot enter the aqueous spaces within the surfactant aggregate. This generates a concentration difference between the inside and outside of the aggregate, which in turn generates an osmotic pressure difference that causes dehydration of the aggregate. With no albumin or polymers in the solution, Curosurf has a bilayer d-spacing of $\sim$11 nm, which decreases to $\sim$6 nm at the highest applied osmotic pressure difference. From Fig. 9, there is an exponential decrease in the d-spacing of the surfactant bilayers with osmotic pressure difference (proportional to the polymer concentration) (67). The applied osmotic pressure difference is balanced against the interbilayer repulsion, which determines the d-spacing. The characteristic decay length of the line fitted to the data $0.72 \pm .02$ nm (67). The characteristic length for electrostatic double-layer repulsion between the bilayers is the Debye length, K. K is inversely proportional to the square root of the ionic strength of the solution (80): $K = (.304/\sqrt{I})$ nm and

$I = 1/2\sum\rho_i Z_i^2 \approx .154$ mol/liter. ρ_i is the molar concentration of each ion, and Z_i is the charge on that ion. This gives $K = .77$ nm for the buffer used in these experiments. Any additional counterions from the anionic lipids in the surfactant (or albumin) increase the ionic strength and further reduces K. The agreement between the experimental decay length and the Debye length of the solution is good and is typical for fluid bilayers with a significant fraction of charged lipids (see Table 1) (67,69).

Also plotted in Fig. 9 is the effect of increasing albumin concentrations on the d-spacing, as well as mixtures of albumin and polymer. When the albumin concentration is expressed as the equivalent osmotic pressure, the d-spacings of the Curosurf aggregates in albumin or albumin plus polymer fall on the same line as for polymer alone. Albumin also acts as an osmotic agent and cannot enter into the aqueous spaces of the surfactant aggregates (Fig. 10). For the 2 mg/ml albumin that inactivates surfactant, the osmotic pressure ($<10^3$ dynes/cm^2) is not sufficient to alter the d-spacing of Curosurf, which is why the freeze-fracture images of Curosurf with 2 mg/ml albumin are unchanged from Curosurf in buffer whereas higher albumin concentrations act similarly to higher PEG concentrations.

Adding 5 wt % 10 kDa PEG to Infasurf also led to dehydration of the surfactant aggregates and a decrease in the bilayer spacing. Fig. 11 shows that the PEG caused the
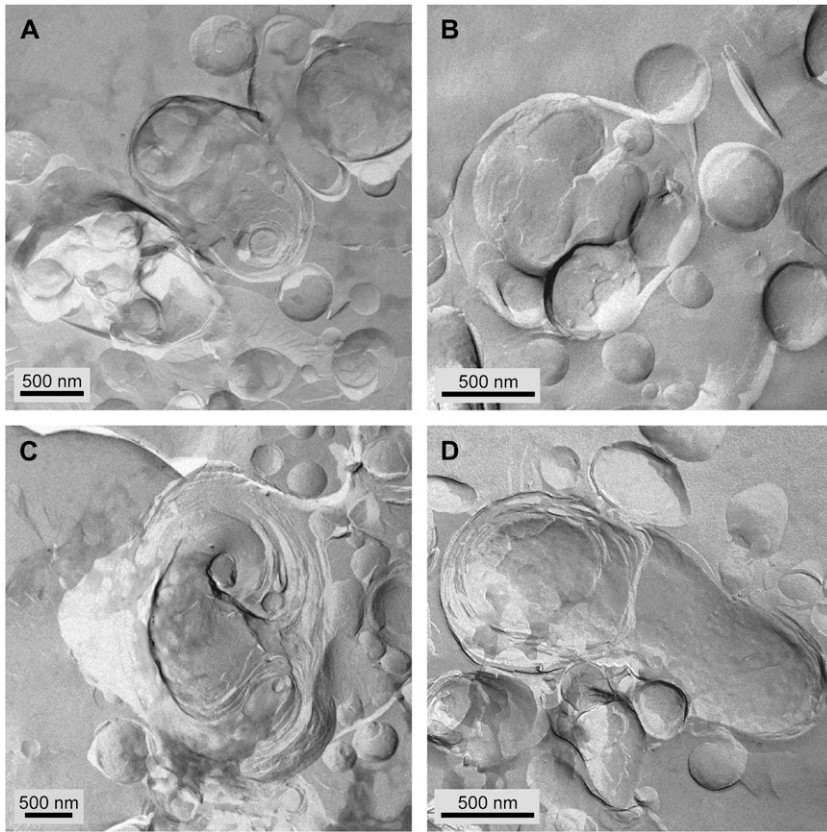
FIGURE 5 FFTEM images of 10 mg/ml Curosurf with bovine serum albumin (BSA) at different concentrations, quenched from room temperature. (A) $c_{BSA} = 0.5$ mg/ml. (B) $c_{BSA} = 1$ mg/ml. (C) $c_{BSA} = 2$ mg/ml. (D) $c_{BSA} = 5$ mg/ml. Adding BSA at different concentrations did not change the aggregate structures in comparison to Fig. 1. The microstructure of the aggregates was multilamellar with interior voids and water pockets and poorly correlated bilayers as in Fig. 1. The size distribution of the aggregates was unchanged and ranged 0.5–3 microns.

Infasurf vesicles to aggregate and fuse. Instead of the vesicle within vesicle structure common when there was no PEG (Fig. 2), the Infasurf aggregates are much more compact with concentric, onion-like bilayer structures. The void spaces and water pockets were removed and the interior compartments have fused. Small angle x-ray diffraction showed that the d-spacing of the Infasurf bilayers decreased from ~7.8 nm with no PEG to ~7.1 nm with 5 wt % PEG. The diffraction peaks changed from weak and diffuse with no PEG (typical of poorly correlated bilayers (as in Fig. 2)) to strong, sharp peaks (not shown) indicative of well-correlated bilayers consistent with Fig. 11. The amount of water within each aggregate was significantly reduced. Survanta, which consisted of compact bilayers with no void spaces, did not show any overall morphological effects caused by adding PEG at 5 wt % (not shown). However, the bilayer spacing also decreased as measured by small angle x-ray from ~7.8 nm with no PEG to ~7.5 nm with 5 wt % PEG. At 5 wt % PEG, the bilayer spacing of Curosurf is ~7.5 nm. All of the clinical surfactants had similar bilayer arrangements in 5 wt % PEG.

Fig. 12 shows the effects of 0.25 wt % 250 kDa HA on the microstructure of Infasurf. There is little difference between the Infasurf aggregates with or without HA (compare Fig. 12 to Fig. 2). This is not surprising as the osmotic pressure of the HA solution is only $\sim 10^3$ dynes/cm^2, compared to the $10^{5.1}$ dynes/cm^2 of the 5 wt % 10 kDa PEG solution. HA, like PEG, does not appear to adsorb to the Infasurf bilayers.

Surface activity

Table 2 shows surface activities of the four surfactants without serum inactivation measured with the PBS. All the surfactants reached a minimum surface tension below 4 mN/m after 5 min of cycling with or without added polymer. Added polymer did decrease the change in bubble size necessary for surface tension to fall to 10 mN/m, ΔA_{10}. ΔA_{10} decreased by 38% when PEG or HA was added to Survanta and by 36% when dextran or HA was added to Curosurf. This suggests increased surfactant adsorption to the bubble in the presence of polymers (17,18). The maximum surface tensions were unaffected by addition of polymer.

Table 3 shows the surface activities of the four surfactants after serum inactivation in the presence and absence of PEG, HA, or dextran. Before adding the polymers, none of the clinical surfactants or native surfactant could reach a minimum surface tension of 10 mN/m on the 10th cycle or even after 5 min of cycling. Serum clearly inactivates all of the clinical surfactants as well as native surfactant under these conditions. After 5 min of cycling, Survanta, Curosurf, and Infasurf all had minimum surface tensions that were lower than control values when PEG, HA, or dextran was added. However, native surfactant only showed a reduction in minimum surface tension when HA was added. Maximum surface tensions were higher for the clinical surfactants than for native surfactant (37–41 vs. 26 mN/m) and were unaffected
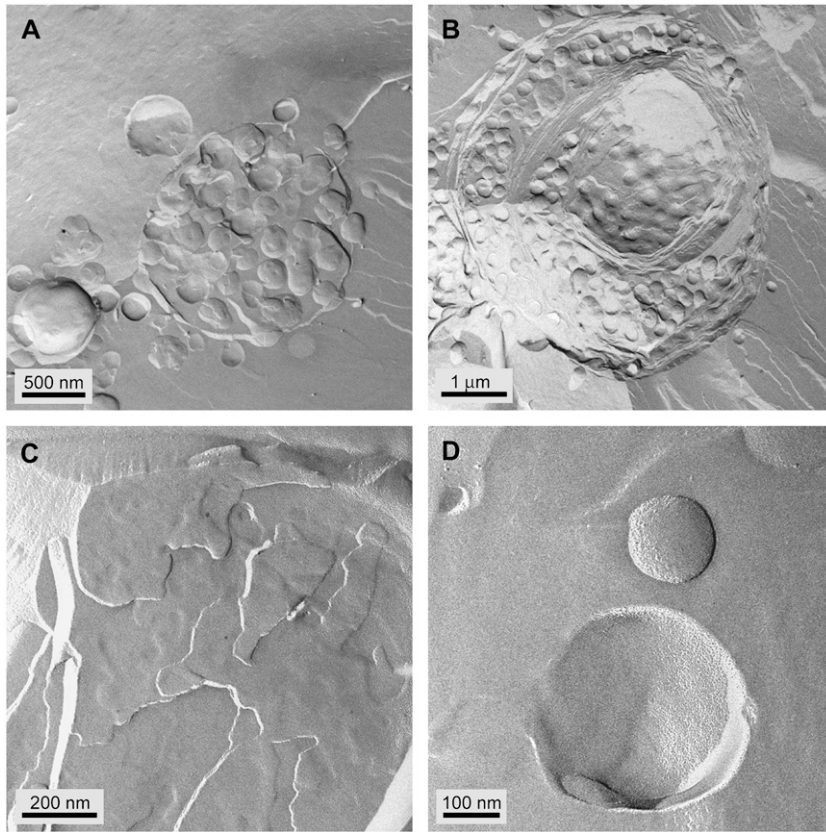
FIGURE 6 FFTEM images of Infasurf (*A*, *B*) and Survanta (*C*, *D*) at 10 mg/ml after adding bovine serum albumin (BSA) at a concentration of 2 mg/ml, quenched from room temperature. Adding BSA did not change the aggregate structures of either formulation. (*A*, *B*) Infasurf showed small, fairly monodisperse vesicles and densely packed vesicle aggregates. The bilayer surfaces were smooth, indicating no adsorption or perturbation by the albumin. (*C*, *D*) Survanta primarily formed stacks of bilayer sheets and only a few small vesicles with no evidence of albumin adsorption (see Figs. 2 and 3).

by addition of serum. PEG decreased the maximum surface tension for Survanta, Curosurf, and Infasurf, and dextran decreased the maximal surface tension for Curosurf and native surfactant.

By definition, none of the four surfactants had a $\Delta A_{10} < 47$ after addition of serum as the minimum surface tension was >10 mN/m. When PEG, HA, or dextran was added to the clinical surfactants, ΔA_{10} decreased, although generally not to the level for surfactants with no serum (Table 2). Effects on ΔA_{10} were most evident with HA for all surfactants except Infasurf. However, all of the polymers led to improved performance of the clinical surfactants and at least

partial reversal of inactivation. There were small differences between the polymer/clinical surfactant combinations; however, the surfactant/polymer ratios examined were not optimized, so these small variations are not unexpected.

DISCUSSION

FFTEM shows that the composition differences between these clinical surfactants (Table 1) are manifested in the microstructure and bilayer organization of the dispersed surfactants. Survanta has the largest aggregates with the best-ordered bilayers: there are no water pockets or voids within

TABLE 2   Data for four surfactants are shown with and without added polymer

	Survanta				Curosurf			
		PEG	dextran	HA		PEG	dextran	HA
ST_{min} (mN/m) 10th cycle	4 ± 0.5	2 ± 1*	3 ± 0.7	1 ± 0*	12 ± 1	13 ± 2	3 ± 1*	8 ± 0.4
ST_{min} (mN/m) 5 min	4 ± 0.6	1 ± 1*	2 ± 0.7*	1 ± 0.2*	4 ± 1	3 ± 1	0.4 ± 0.4*	0.2 ± 0.2*
A_{10} (% area reduction)	21 ± 3	13 ± 1*	19 ± 2	13 ± 1*	22 ± 2	18 ± 2	14 ± 1*	14 ± 2*
	Infasurf				Native surfactant			
		PEG	dextran	HA		PEG	dextran	HA
ST_{min} (mN/m) 10th cycle	15 ± 1	13 ± 1	9 ± 2*	10 ± 2	17 ± 1	12 ± 1*	9 ± 2	9 ± 1*
ST_{min} (mN/m) 5 min	5 ± 1	6 ± 1	3 ± 2	2 ± 1*	2 ± 0.7	6 ± 2	3 ± 1	0 ± 0*
A_{10} (% area reduction)	28 ± 1	24 ± 1	22 ± 1*	18 ± 3*	22 ± 2	16 ± 2	18 ± 2	14 ± 2*

ST_{min}, minimal surface tension during cycling. Area reduction (ΔA_{10}) after 5 min of cycling without serum inactivation.
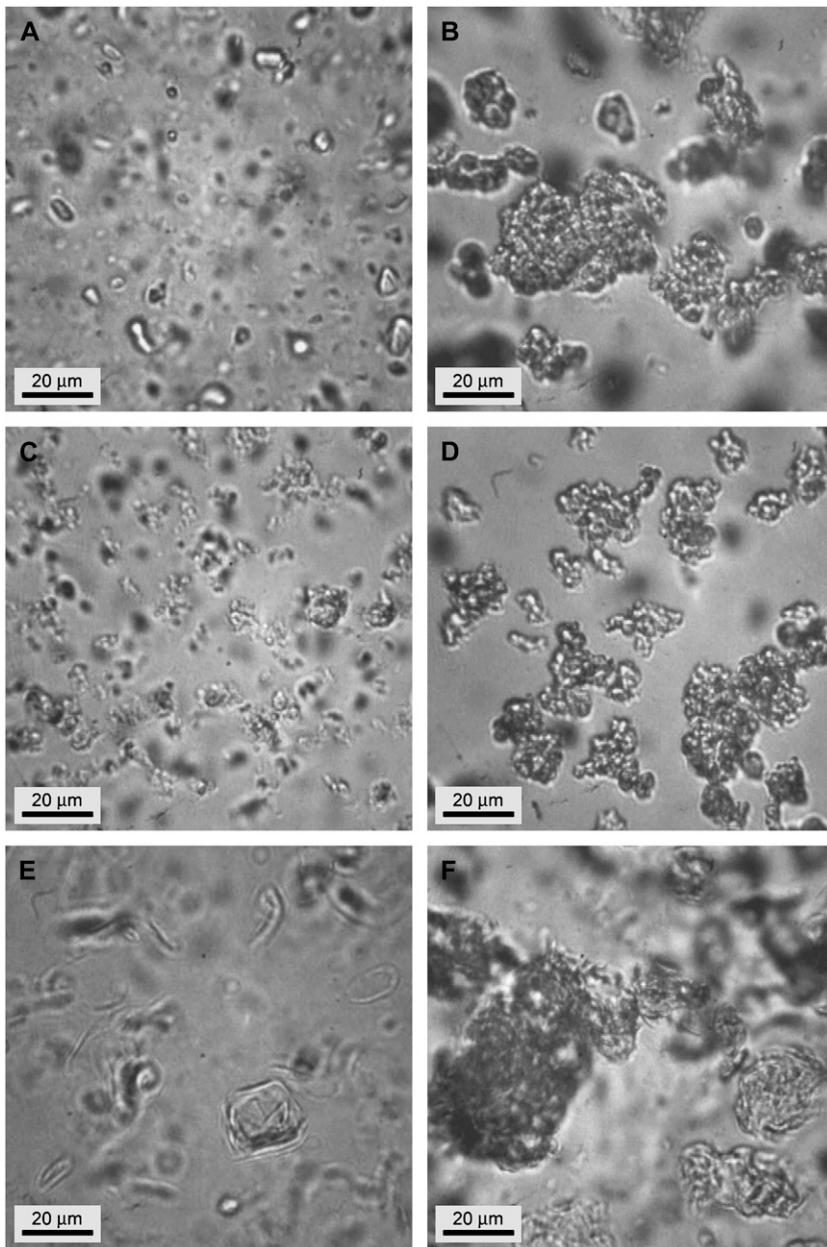*$p < 0.05$, estimated by ANOVA corrected for multiple comparisons.

FIGURE 7 Optical phase contrast microscopy images of Curosurf (*A*, *B*), Infasurf (*C*, *D*), and Survanta (*E*, *F*) before and after 5 wt% 10 kDa PEG addition. (*A*, *C*, *E*) Without PEG, all of the clinical surfactants consisted of dispersed, small aggregates (*B*, *D*, *F*). Adding PEG induced flocculation of the small aggregates and formed large agglomerations of up to 100 μm. These large flocs could be redispersed by gentle agitation, indicating that the forces holding the flocs together were reversible, which is typical for depletion attraction (18,79).

the aggregates. This is to be expected from the large fraction of saturated DPPC and palmitic acid in Survanta (Table 1), these bilayers are in the semicrystalline gel, L_β phase at room, and body temperature (62,76,81,82). Such gel phase bilayers pack better than more fluid, L_α phase bilayers, as the bilayers undergo smaller thermal fluctuations due to their increased rigidity (83–88).

Curosurf is intermediate in the fraction of saturated lipids, leading to more poorly ordered bilayers and water pockets within the aggregates. Small angle x-ray scattering shows that the bilayer spacing is determined by repulsive electrostatic double layer forces and the d-spacing is consistent with fluid L_α phase bilayers with a strong repulsive electrostatic interaction and large thermal fluctuations (67,69). The bilayer

spacing is rather poorly defined and the bilayers are not well ordered.

As received, Infasurf has the most unusual aggregates, consisting of small unilamellar vesicles trapped within an enclosing bilayer membrane. The interior of the particles is full of water pockets and voids. This structure is not typical of simple lipid dispersions and may be due to the fact that Infasurf is the only one of these clinical surfactants to contain cholesterol (74).

The primary effect of albumin and polymer on the microstructure of the clinical lung surfactants is via osmotic pressure. Many macromolecules cannot penetrate bilayer aggregates, resulting in a concentration difference between the interior aqueous compartments of the surfactant aggregate
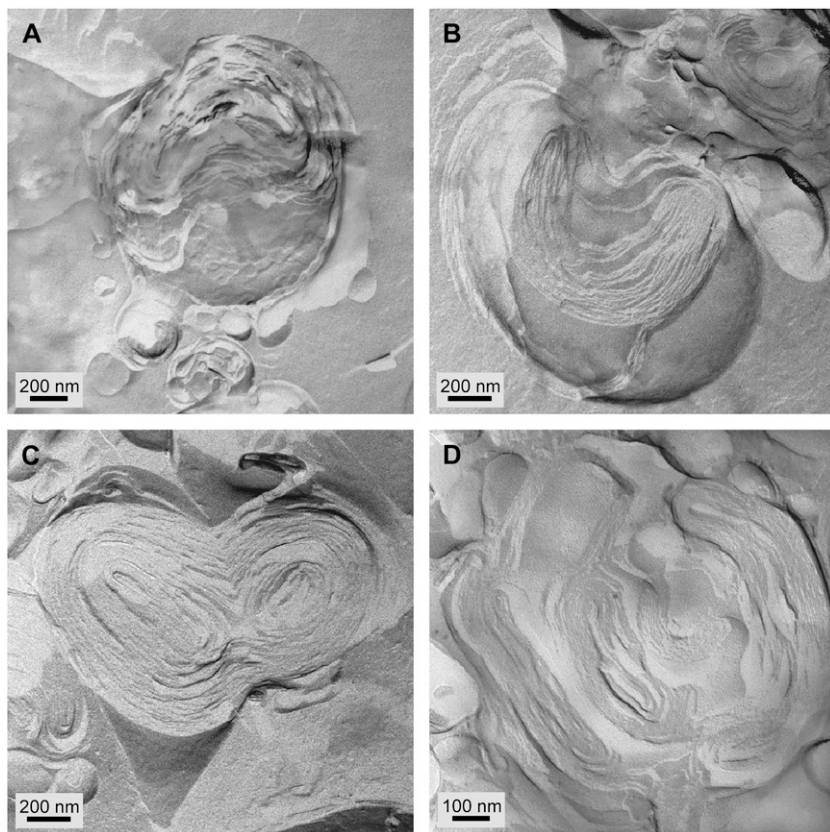
FIGURE 8 FFTEM images of 10 mg/ml Curosurf after adding 5 wt % 10 kDa PEG at different concentrations. (A) $c_{PEG} = 1$ wt %. (B) $c_{PEG} = 5$ wt %. (C) $c_{PEG} = 10$ wt %. (D) $c_{PEG} = 20$ wt %. As in the optical images (Fig. 7), the PEG caused flocculation of the surfactant aggregates. In addition, there appeared to be fusion of the smaller vesicles and the bilayers became better ordered within the aggregates. The pockets of water and void spaces were eliminated at the higher PEG fractions. This is consistent with the PEG acting as a nonpenetrating osmotic agent that dehydrates the surfactant aggregates.

and the bulk solution. Such a concentration difference generates an osmotic pressure difference proportional to the polymer/albumin concentration and inversely proportional to the polymer molecular weight. At concentrations sufficient to inhibit surfactant, freeze-fracture TEM images show that albumin does not significantly alter the structure of any of the clinical surfactants. Hence, it is clear that microstructural changes to the surfactant in the suspension are not responsible for surfactant inactivation in vitro. The osmotic pressure of the low molecular weight PEG solutions capable of reversing inactivation are sufficiently high that the microstructure of Curosurf and Infasurf are significantly altered. The PEG (or high albumin concentrations) dehydrates the aggregates, leading to a removal of the interior water pockets and voids in the aggregates and a decrease in the bilayer spacing. The morphology of Survanta, which has relatively well-ordered bilayers, is not affected by PEG, although the bilayer spacing does decrease as in Curosurf and Infasurf. For 5 wt % PEG, all three clinical surfactants are onion-like, with well-ordered bilayers; the d-spacings range 7.1–7. 5 nm. In contrast, the lower concentrations of the higher molecular weight HA that reverse inactivation do not alter the microstructure of even Infasurf, the surfactant most affected by PEG. The osmotic pressure of the HA solution is simply too low to alter the microstructure.

However, PBS experiments showed that all three clinical surfactants were inactivated by serum, and adding any one of the polymers tested reversed inactivation. There were small variations between the pairs of surfactant/polymer in the minimum surface tension and the area changes required to reach a low surface tension that were likely due to the lack of optimization of conditions for each pair. However, there was no correlation between the microstructure changes in the surfactant aggregates and the extent of inhibition reversal. HA, which did not alter the surfactant microstructure, was, in general, more effective at inhibition reversal than PEG or dextran. The lack of correlation between surfactant inactivation or reversal and surfactant microstructure alteration refutes the hypothesis that inactivation or inactivation reversal is due to changes in the bilayer organization.

Although the osmotic forces can be sufficient to alter the bilayer organization, the differences in energy are likely to be insufficient to influence the amount of surfactant at the interface. The change in the chemical potential, $\Delta\mu$, per molecule in the bilayer due to the applied osmotic pressure, Π_{os}, is given by the work done by the osmotic pressure in changing the volume of the surfactant (67):

$$\Delta\mu = -\Pi_{os}\Delta V$$

ΔV is the change in volume due to the change in osmotic pressure. From Fig. 9, the maximum change in d-spacing is ~5 nm for an applied osmotic pressure of 10^6 dynes/cm^2. Assuming an average area per molecule of 0.5 nm^2 for lipids, the change in volume per molecule due to the osmotic
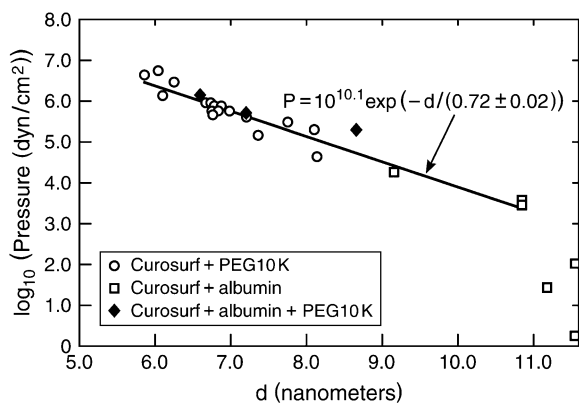
FIGURE 9 Bilayer d-spacing measured by small angle x-ray scattering from dispersions of Curosurf, Curosurf plus albumin, and Curosurf plus albumin and PEG polymer as a function of the osmotic pressure of polymer or polymer plus albumin. For osmotic pressures $>10^3$ dynes/cm^2, the d-spacing decreases exponentially with increasing osmotic pressure with a decay length of 0.72 nm, which is nearly identical to the calculated Debye length of the solvent. The albumin and polymer act primarily as osmotic agents that dehydrate the bilayers, as in the TEM images. This confirms that albumin and polymer do not adsorb to or penetrate the surfactant aggregates.

pressure is ~1.25 nm^3 (there are two molecules per bilayer). As a result, the net change in chemical potential is 1.25×10^{-15} ergs/molecule, which should be compared to the thermal energy, k_BT, of $\sim 4 \times 10^{-14}$ ergs/molecule. Hence, the osmotic pressure alters the chemical potential $<.06$ k_BT, so the change in conversion between bilayer and monolayer, which likely depends on differences in the chemical potential of individual surfactant molecules in monolayers or bilayers, should not be affected.

PEG, dextrans, and HA are all approved in various forms for internal use in humans by the Federal Drug Administration. PEG is a linear or branched neutral polymer with the general formula $H(OCH_2CH_2)_nOH$. When used in high concentrations it acts as a cellular fusagen (89). This is consistent with the effects we observe on both Curosurf and Infasurf bilayer aggregates at high PEG concentrations. The osmotic pressure of the PEG is sufficient to cause fusion and

reorganization of the bilayers in the aggregates, along with a decrease in the bilayer spacing.

HA differs from PEG and dextran in several respects. HA is an ionic, nonsulfated polymer of N-acetyl-glucosamine linked β-1, 4 to glucuronic acid which is linked β-1, 3 to N-acetylglucosamine. HA serves many different roles in the body, depending largely on its molecular weight. For example, high molecular weight HA aids in the lubrication of joints and comprises filler material for the vitreous humor of the eye and the umbilical cord of the fetus. Low molecular weight forms are agonists for intracellular processes as diverse as inflammation or normal differentiation (90). In the lungs, HA and other glycosaminoglycans are secreted by alveolar epithelial cells (91,92). HA in normal rat broncho-alveolar lavage has a molecular mass of ~220 kDa (93), much lower than that of the lung interstitium (~3000 kDa) (94). In alveolar subphase fluid, HA is reported to have a concentration of ~4000 μg/L based on estimates from bronchoalveolar lavage (93). These may be underestimates because of inefficiency of removal of protein-bound HA and because of uncertainty in estimating subphase volumes. Several beneficial effects have been reported for HA in the air spaces or airways. Aerosolization of HA (~100 kDa) into the lungs does not cause histological inflammation, and its use decreases risk of elastase-induced or smoking-induced experimental emphysema (95,96). Forteza and co-workers find that endogenous HA stimulates airway ciliary action and may serve to enhance airway defenses (97). Nitzan and co-workers report that HA decreases phospholipase degradation of liposomes (98). Additional proposed beneficial effects relate to cystic fibrosis, asthma, or injury from bleomycin or tobacco smoke (90).

As PEG, dextran, HA, etc. have little in common chemically but all reverse inhibition in all clinical surfactants, a physical explanation for surfactant inhibition reversal seems more likely than one that depends on specific chemical interactions between polymers and surfactants. One possibility recently advanced is that serum inactivation is due to competitive adsorption of surface-active proteins at the air-water interface and that polymer-induced inactivation reversal is
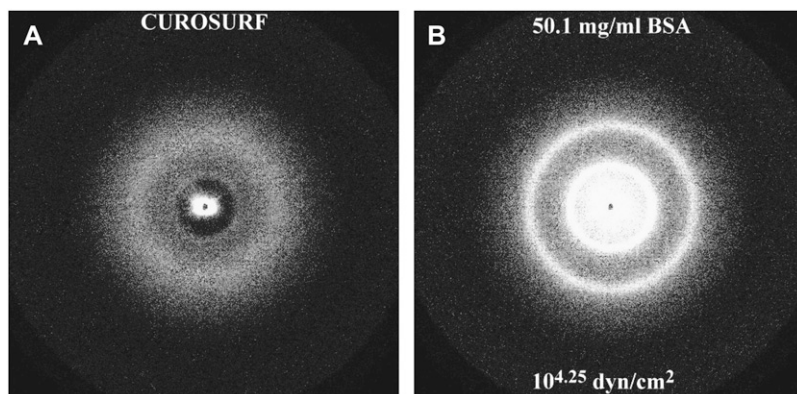

FIGURE 10 Small angle x-ray diffraction of Curosurf (A) as received and (B) with 50.1 mg/ml bovine serum albumin, which is equivalent to an osmotic pressure of $10^{4.25}$ dynes/cm^2. As received, the single bilayer reflection from Curosurf is broad, indicative of poorly organized bilayers as in Fig. 8 A. After dehydration and rearrangement due to the osmotic pressure induced by the added BSA, the bilayer spacing has decreased and the order of the bilayers has increased, as shown by the much sharper reflections along with the appearance of the second reflection.
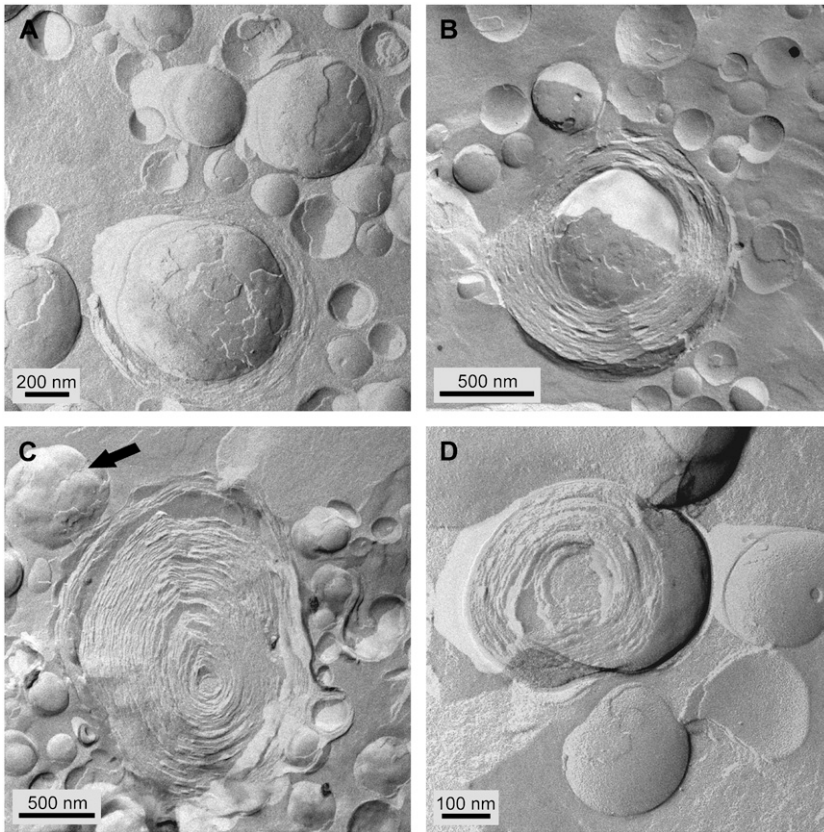
FIGURE 11 FFTEM images of 10 mg/ml Infasurf after adding 5 wt % 10 kDa PEG. (*A–D*) The PEG caused the Infasurf aggregates to compact and dehydrate; there were no longer vesicle within vesicle structures, but rather onion-like multilamellar particles. The small vesicles appear to bind to and fuse with the larger particles (*arrows*).

due to elimination of the energy barrier to adsorption via the so-called ''depletion attraction'' (17,18,78). In a suspension-containing particles of different sizes, there is an attraction between the larger particles (the surfactant aggregates) due to the excluded volume that becomes available to the smaller particles (the polymer molecules) when the larger particles approach one another, a wall, or an interface (79,99). The range of the attraction between the large particles is roughly the diameter of the small particles, as the small particle concentration becomes ''depleted'' when the gap between the large particles is too small for the small particles to fit. Depleting

the small particles in the gaps generates an osmotic pressure between the large particles, leading to an attractive force between the large particles. In the biological literature, depletion attraction is also known as ''macromolecular crowding'' (100). The depletion attraction is known to cause colloidal particles to flocculate in solution (see Fig. 7) (79,99,101) and concentrate and order at interfaces (99,101–103). The depletion attraction arises for any nonadsorbing polymer in a colloidal suspension, and the net attractive force is proportional to the molecular weight and the polymer concentration. Recent work has shown that the depletion attraction can enhance
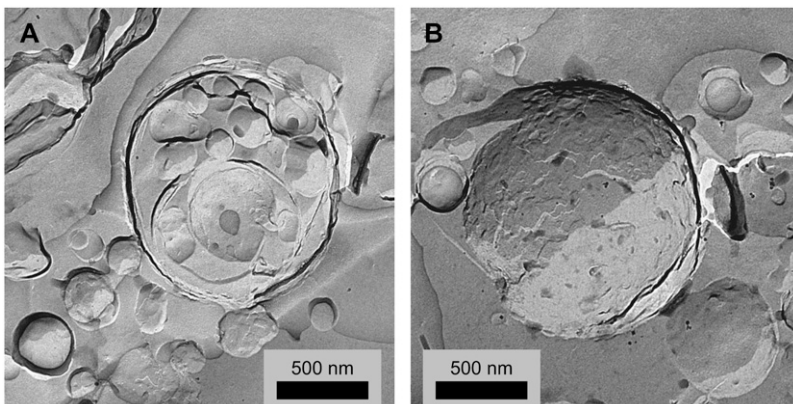

FIGURE 12 FFTEM images of 10 mg/ml Infasurf after adding 0.25 wt % 250 kDa HA. (*A, B*) The HA caused minimal variation in the microstructure of the Infasurf particles. The open vesicle within a vesicle structure seen in Fig. 2 is retained. Compare to the onion-like structures in Fig. 11. Many of the small vesicles remain unfused. The lower osmotic pressure of the HA is not sufficient to cause significant rearrangement of the Infasurf bilayers.

TABLE 3 Data for four surfactants are shown with and without added polymer after addition of serum used as an inactivating substance; data for four surfactants are shown with and without added polymer

	Survanta				Curosurf			
		PEG	dextran	HA		PEG	dextran	HA
ST_{min} (mN/m) 10th cycle	27 ± 2	3 ± 1*	13 ± 2*	7 ± 1*	19 ± 0.5	14 ± 1*	13 ± 2*	8 ± 0.4*
ST_{min} (mN/m) 5 min	20 ± 2	1 ± 1*	2 ± 1*	4 ± 0.2*	18 ± 0.5	9 ± 2*	2 ± 1*	0.2 ± 0.2*
A_{10} (% area reduction)	>47	19 ± 1	29 ± 1	21 ± 1	>47	33 ± 5	18 ± 4	18 ± 2
	Infasurf				Native surfactant			
		PEG	dextran	HA		PEG	dextran	HA
ST_{min} (mN/m) 10th cycle	19 ± 1	15 ± 1	9 ± 2*	17 ± 0.5	18 ± 1	16 ± 1	17 ± 1	11 ± 2*
ST_{min} (mN/m) 5 min	16 ± 1	11 ± 1	5 ± 2*	2 ± 1*	14 ± 0.5	14 ± 0.9	11 ± 3	2 ± 1*
A_{10} (% area reduction)	>47	41 ± 6	30 ± 6	25 ± 2	>47	45 ± 2	34 ± 5	16 ± 3

the adsorption of large particles (such as surfactant aggregates) to interfaces already covered with smaller particles (albumin or serum proteins) (17,18,78). In addition to providing a mechanism of inhibition reversal, macromolecules, particularly hyaluronan (HA), that naturally exist in the alveolar spaces (90) may assist in the normal adsorption of lung surfactant to the alveolar interface.

CONCLUSIONS

FFTEM of the clinical lung surfactants Survanta, Curosurf, and Infasurf (FFTEM) shows significant differences in the bilayer organization of the as received materials. The major difference is the fraction of water within the bilayer aggregates, which increases from Survanta to Curosurf to Infasurf. Although each clinical surfactant has its own distinct bilayer organization, freeze-fracture images show that albumin and polymers do not adsorb to any of the clinical surfactant aggregates. Rather, both albumin and polymers act to dehydrate the surfactant aggregates by creating an osmotic pressure between the interior of the aggregate and the exterior. The aggregates expel any interior pockets of water and form well-ordered bilayers, with an interlayer spacing that depends on the osmotic pressure of the polymer or albumin solution. There is clear evidence of fusion of smaller aggregates to form larger aggregates, in addition to the flocculation observed via optical microscopy. Small angle x-ray scattering shows that the d-spacings of Curosurf, Infasurf, and Survanta depend on the osmotic pressure, consistent with the polymer and albumin not being able to access the interior of the aggregates (67).

Albumin, polymers, and their mixtures alter the surfactant aggregate microstructure in the same manner; this implies that albumin does not inactivate surfactant by alterations in surfactant microstructure. In addition, the microstructure alterations of PEG and other polymers do not themselves reverse surfactant inactivation. This has been shown by comparing the effects of 5 wt % 10 kDa PEG with 0.25 wt % 250 kDa HA on surfactant microstructure and surfactant inactivation. These polymer concentrations are sufficient to reverse inactivation of the clinical surfactants; the lower HA concentration actually provides more complete inactivation reversal than does the higher PEG concentration in pulsating bubble experiments. However, the PEG solution has an osmotic pressure more than 100 times higher than the HA solution. FFTEM and small angle x-ray scattering show that high concentration of PEG necessary to reverse inhibition significantly alters the bilayer organization of the surfactant aggregates, whereas the lower concentrations of HA do not. In addition, the bilayer morphology of Survanta is minimally altered by PEG, whereas Infasurf and Curosurf aggregates undergo extensive reorganization, yet inactivation reversal occurs in all of the clinical surfactants. Hence, alternate mechanisms must be responsible for both inhibition of surfactant by surface active proteins and the polymer-induced inhibition reversal of clinical surfactants.

REFERENCES

1. Clements, J. A., and M. E. Avery. 1998. Lung surfactant and neonatal respiratory distress syndrome. *Am. J. Respir. Crit. Care Med.* 157: 59–66.

2. Zasadzinski, J. A., J. Ding, H. E. Warriner, F. Bringezu, and A. J. Waring. 2001. The physics and physiology of lung surfactants. *Curr. Opinion Coll. Int. Sci.* 6:506–513.

3. Avery, M. E. 2000. Surfactant deficiency in hyaline membrane disease. *Am. J. Respir. Crit. Care Med.* 161:1074–1075.

4. Notter, R. H. 2000. Lung Surfactant: Basic Science and Clinical Applications. Marcel Dekker, New York.

5. Suresh, G. K., and R. F. Soll. 2005. Overview of surfactant replacement trials. *J. Perinatol.* 25:S40–S44.

6. Spragg, R. G., J. F. Lewis, H. D. Walmrath, J. Johannigman, G. Bellingan, P. F. Laterre, M. C. Witte, G. A. Richards, G. Rippin, G. Rathgeb, D. Hafner, F. J. Taut, and W. Seeger. 2004. Effect of recombinant surfactant protein C-based surfactant on the acute respiratory distress syndrome. *N. Engl. J. Med.* 351:884–892.

7. Gregory, T., and K. Steinberg. 1997. Bovine surfactant therapy for patients with acute respiratory distress syndrome. *Am. J. Respir. Crit. Care Med.* 155:1309–1315.

8. Spragg, R. J., and R. M. Smith. 1998. Surfactant replacement in patients with ARDS: result of clinical trials. *In* Acute Respiratory Distress Syndrome: Cellular and Molecular Mechanisms and Clinical Management, vol. 297. S. Matalon and J. I. Sznajder, editors. Plenum Press, New York. 107–116.

9. Lu, K. W., H. William Taeusch, B. Robertson, J. Goerke, and J. A. Clements. 2000. Polymer-surfactant treatment of meconium-induced acute lung injury. *Am. J. Respir. Crit. Care Med.* 162:623–628.

10. Tashiro, K., T. Kobayashi, and B. Robertson. 2000. Dextran reduces surfactant inhibition by meconium. *Acta Paediatr.* 89:1439–1445.

11. Tashiro, K., X. G. Cui, T. Kobayashi, T. Curstedt, and B. Robertson. 2003. Modified protocols for surfactant therapy in experimental meconium aspiration syndrome. *Biol. Neonate.* 83:49–56.

12. Holm, B. A., G. Enhorning, and R. H. Notter. 1988. A biophysical mechanism by which plasma proteins inhibit lung surfactant activity. *Chem. Phys. Lipids.* 1988:49–55.

13. Taeusch, H. W. 2000. Treatment of acute (adult) respiratory distress syndrome: the holy grail of surfactant therapy. *Biol. Neonate.* 77(suppl. 1):2–8.

14. Lu, J. J., W. W. Y. Cheung, L. M. Y. Yu, Z. Policova, D. Li, M. L. Hair, and A. W. Neumann. 2002. The effect of dextran to restore the activity of pulmonary surfactant inhibited by albumin. *Respir. Physiol. Neruobiol.* 130:169–179.

15. Lu, J. J., L. M. Y. Yu, W. W. Y. Cheung, Z. Policova, D. Li, M. L. Hair, and A. W. Neumann. 2003. The effect of concentration on the bulk adsorption of bovine lipid extract surfactant. *Colloids Surf. B. Biointerfaces.* 29:119–130.

16. Lu, K., H. W. Taeusch, B. Robertson, J. Goerke, and J. A. Clements. 2001. Polyethylene glycol/surfactant mixtures improve lung function after HCl and endotoxin lung injuries. *Am. J. Respir. Crit. Care Med.* 164:1531–1536.

17. Taeusch, H. W., J. Bernadino de la Serna, J. Perez-Gil, C. Alonso, and J. A. Zasadzinski. 2005. Inactivation of pulmonary surfactant due to serum-inhibited adsorption and reversal by hydrophilic polymers: experimental. *Biophys. J.* 89:1769–1779.

18. Zasadzinski, J. A., T. F. Alig, C. Alonso, J. Bernadino de la Serna, J. Perez-Gil, H. W. Taeusch. 2005. Inhibition of pulmonary surfactant adsorption by serum and the mechanisms of reversal by hydrophilic polymers: theory. *Biophys. J.* 89:1621–1629.

19. Lu, K., J. Goerke, J. A. Clements, and H. W. Taeusch. 2005. Hyaluronan reduces surfactant inactivation in vitro. *Pediatr. Res.* 57:237–241.

20. Lu, J. J., L. Yu, W. W. Y. Cheung, I. Goldthorpe, Y. Zuo, Z. Policova, P. Cox, and A. W. Neumann. 2005. PEG enhances dynamic surface activity of a bovine lipid extract surfactant (BLES). *Colloids Surf. B. Biointerfaces.* 41:145–151.

21. Zuo, Y. Y., H. Alolabi, A. Shapel, N. Kang, Z. Policova, P. N. Cox, E. Acosta, M. L. Hair, and A. W. Neumann. 2006. Chitosan enhances the in vitro surface activity of dilute lung surfactant preparations and resists albumin-induced inactivation. *Pediatr. Res.* 60:125–130.

22. Kobayashi, T., K. Ohta, K. Tashiro, K. Nishizuka, W.-M. Chen, S. Ohmura, and K. Yamamoto. 1999. Dextran restores albumin-inhibited surface activity of pulmonary surfactant extract. *J. Appl. Physiol.* 86:1778–1784.

23. Lu, K., J. Goerke, J. A. Clements, and H. W. Taeusch. 2005. Hyaluronan reduces surfactant inhibition and improves rat lung function after meconium lung injury. *Pediatr. Res.* 58:206–210.

24. Lu, K., B. Robertson, and H. W. Taeusch. 2005. Dextran or polyethylene glycol added to Curosurf for treatment of meconium lung injury in rats. *Biol. Neonate.* 88:46–53.

25. Hyers, T. M. 1991. Adult respiratory distress syndrome: definition, risk factors and outcome. *In* Adult Respiratory Distress Syndrome, vol. 50. W. M. Zapol and F. Lemaire, editors. Marcel Dekker, New York. 23–33.

26. Anzueto, A. 2002. Surfactant supplementation in the lung. *Respir. Care Clin. N. Am.* 2:211–236.

27. Spragg, R. G. 1991. Abnormalities of lung surfactant function in patients with acute lung injury. *In* Adult Respiratory Distress Syndrome, vol. 50. W. M. Zapol and F. Lemaire, editors. Marcel Dekker, New York. 381–395.

28. McIntyre, R. C. Jr., E. J. Pulido, D. D. Bensard, B. D. Shames, and E. Abraham. 2000. Thirty years of clinical trials in acute respiratory distress syndrome. *Crit. Care Med.* 28:3314–3331.

29. Ishizaka, A., T. Matsuda, K. Albertine, H. Koh, S. Tasaka, N. Hasegawa, N. Kohno, T. Kotani, H. Morisakai, J. Takeda, M. Nakamura, X. Fang, T. Martin, M. Matthay, and S. Hashimoto. 2004. Elevation of KL-6, a lung epithelial cell marker, in plasma and epithelial lining fluid in acute respiratory distress syndrome. *Am. J. Physiol. Lung Cell. Mol. Physiol.* 286:L1088–L1094.

30. Warriner, H. E., J. Ding, A. J. Waring, and J. A. Zasadzinski. 2002. A concentration-dependent mechanism by which serum albumin inactivates replacement lung surfactants. *Biophys. J.* 82:835–842.

31. Holm, B. A., R. H. Notter, and J. N. Finkelstein. 1985. Surface property changes from interactions of albumin with natural lung surfactant and extracted lung lipids. *Chem. Phys. Lipids.* 38:287–298.

32. Cockshutt, A. M., J. Weitz, and F. Possmayer. 1990. Pulmonary surfactant-associated protein A enhances the surface activity of lipid extract surfactant and reverses inhibition by blood proteins in vitro. *Biochemistry.* 29:8424–8429.

33. Seeger, W., C. Grube, A. Gunther, and R. Schmidt. 1993. Surfactant inhibition by plasma proteins: differential sensitivity of various surfactant preparations. *Eur. Respir. J.* 6:971–977.

34. Seeger, W., A. Guenther, and C. Thede. 1992. Differential sensitivity to fibrinogen inhibition of SP-C- vs. SP-B-based surfactants. *Am. J. Physiol.* 262:L286–L291.

35. Amirkhanian, J. D., R. Bruni, A. J. Waring, and H. W. Taeusch. 1991. Inhibition of mixtures of surfactant lipids and synthetic sequences of surfactant proteins Sp-B and Sp-C. *Biochim. Biophys. Acta.* 1096: 355–360.

36. Amirkhanian, J. D., R. Bruni, A. J. Waring, C. Navar, and H. W. Taeusch. 1993. Full length synthetic surfactant proteins, Sp-B and Sp-C, reduce surfactant inactivation by serum. *Biochim. Biophys. Acta.* 1168:315–320.

37. Rider, E., M. Ikegami, J. A. Whitsett, W. Hull, D. Absolom, and A. H. Jobe. 1993. Treatment responses to surfactants containing natural surfactant proteins in preterm rabbits. *Am. Rev. Respir. Dis.* 153: 669–676.

38. Strayer, D., E. Herting, B. Sun, and B. Robertson. 1996. Antibody to surfactant protein A increases sensitivity of pulmonary surfactant to inactivation by fibrinogen in vivo. *Am. Rev. Respir. Dis.* 153:1116–1122.

39. Kobayashi, T., K. Tashiro, X. Cui, T. Konzaki, Y. Xu, C. Kabata, and K. Yamamoto. 2001. Experimental models of acute respiratory distress syndrome: clinical relevance and response to surfactant therapy. *Biol. Neonate.* 80:26–28.

40. Cui, X., K. Tashiro, H. Matsumoto, Y. Tsubokawa, and T. Kobayashi. 2003. Aerosolized surfactant and dextran for experimental acute respiratory distress syndrome caused by acidified milk in rats. *Acta Anaethesiol. Scand.* 47:853–860.

41. Yu, L. M. Y., J. J. Lu, I. W. Y. Chiu, K. S. Leung, Y. W. Chan, L. Zhang, Z. Policova, M. L. Hair, and A. W. Neumann. 2004. Polyethylene glycol enhances the surface activity of a pulmonary surfactant. *Colloids Surf. B. Biointerfaces.* 36:167–176.

42. Bae, C., A. Takahashi, S. Chida, and M. Sasaki. 1998. Morphology and function of pulmonary surfactant inhibited by meconium. *Pediatr. Res.* 44:187–191.

43. Schmiedl, A., N. Krug, and J. M. Hohfeld. 2004. Influence of plasma and inflammatory proteins on the ultrastructure of exogenous surfactant. *J. Electron Microsc. (Tokyo).* 53:407–416.

44. Ochs, M., M. Schuttler, G. Stichtenoth, and E. Herting. 2006. Morphological alterations of exogenous surfactant inhibited by meconium can be prevented by dextran. *Respir. Res.* 7:86–95.

45. Hayat, M. 1989. Principles and Techniques of Electron Microscopy: Biological Applications, 3rd ed. CRC Press, Boca Raton, FL.

46. Zasadzinski, J., C. Stratton, and D. Heetderks. 1987. Liquid crystal morphology and defects in in vivo human and mammalian phosphatidylcholine lung multilamellar surfactant. *Langmuir.* 3:592–595.

47. Stratton, C. J., J. A. Zasadzinski, and D. Elkins. 1988. Lung lamellar body amphiphilic topography: a morphological evaluation using the continuum theory of liquid crystals: I. Closed surfaces: closed spheres, concentric tori, and Dupin cyclides. *Anat. Rec.* 221:503–519.

48. Zasadzinski, J. A., C. J. Stratton, and R. Rudolph. 1988. Lung lamellar body amphiphilic topography: a morphological evaluation using the continuum theory of liquid crystals: II. Disclinations, edge dislocations, and irregular defects. *Anat. Rec.* 221:520–532.

49. Zasadzinski, J. A., and S. M. Bailey. 1989. Applications of freeze-fracture replication to problems in materials and colloid science. *J. Electron Microsc. Tech.* 13:309–334.

50. Zasadzinski, J. A., L. E. Scriven, and H. T. Davis. 1985. Liposome structure and defects. *Philos. Mag. A.* 51:287–302.

51. Spector, M. S., J. A. Zasadzinski, and M. B. Sankaram. 1996. Topology of multivesicular liposomes, a model biliquid foam. *Langmuir.* 12:4704–4708.

52. Keller, S. L., P. Boltenhagen, D. J. Pine, and J. A. Zasadzinski. 1998. Direct observation of shear induced structures in wormlike micellar solutions by freeze-fracture electron microscopy. *Phys. Rev. Lett.* 80:2725–2728.

53. Keller, S. L., H. E. Warriner, C. R. Safinya, and J. A. Zasadzinski. 1997. Direct observation of a defect mediated viscoelastic transition in a hydrogel of lipid membranes and polymer lipids. *Phys. Rev. Lett.* 78:4781–4784.

54. Walker, S. A., M. T. Kennedy, and J. A. Zasadzinski. 1997. Encapsulation of bilayer vesicles by self-assembly. *Nature.* 387:61–64.

55. Coldren, B. A., R. van Zanten, M. J. Mackel, J. A. Zasadzinski, and H. T. Jung. 2003. From vesicle size distributions to bilayer elasticity via cryo-transmission and freeze-fracture electron microscopy. *Langmuir.* 19:5632–5639.

56. Coldren, B. A., H. E. Warriner, R. van Zanten, J. A. Zasadzinski, and E. B. Sirota. 2006. Zero spontaneous curvature and its effects on lamellar phase morphology and vesicle size distributions. *Langmuir.* 22:2472–2481.

57. Kaler, E. W., A. K. Murthy, B. E. Rodriguez, and J. A. N. Zasadzinski. 1989. Spontaneous vesicle formation in aqueous mixtures of single-tailed surfactants. *Science.* 245:1371–1374.

58. Bailey, S. M., S. Chiruvolu, J. N. Israelachvili, and J. A. Zasadzinski. 1990. Measurements of forces involved in vesicle adhesion using freeze-fracture electron microscopy. *Langmuir.* 6:1326–1329.

59. Zasadzinski, J., J. Schneir, J. Gurley, V. Elings, and P. K. Hansma. 1988. Scanning tunneling microscopy of freeze-fracture replicas of biomembranes. *Science.* 239:1014–1015.

60. Spector, M. S., E. Naranjo, S. Chiruvolu, and J. A. Zasadzinski. 1994. Conformations of a tethered membrane: crumpling in graphitic oxide. *Phys. Rev. Lett.* 73:2867–2870.

61. Sammon, M. J., J. A. Zasadzinski, and M. R. Kuzma. 1986. Electron microscope observation of the smectic-nematic transition in a lyotropic liquid crystal. *Phys. Rev. Lett.* 57:2834–2837.

62. Zasadzinski, J. A., and M. B. Schneider. 1987. Ripple wavelength, amplitude, and configuration in lyotropic liquid-crystals as a function of effective headgroup size. *J. Physique (France).* 48:2001–2011.

63. Zasadzinski, J. A. 1986. TEM observations of sonication induced changes in liposome structure. *Biophys. J.* 49:1119–1130.

64. Bloom, B. T., J. Kattwinkel, R. T. Hall, P. M. Delmore, E. A. Egan, J. R. Trout, M. H. Malloy, D. R. Brown, I. R. Holzman, C. H. Coghill, W. A. Carlo, A. K. Pramanik, M. A. McCaffree, P. L. Toubas, S. Laudert, L. L. Gratny, K. B. Weatherstone, J. H. Seguin, L. D. Willett, G. R. Gutcher, D. H. Mueller, and W. H. Topper. 1997. Comparison of Infasurf (calf lung surfactant extract) to Survanta (Beractant) in the treatment and prevention of respiratory distress syndrome. *Pediatrics.* 100:31–38.

65. Ramanathan, R., M. Rasmussen, D. R. Gerstmann, N. Finer, K. Sekar, and North American Study Group. 2004. A randomized, multicenter masked comparison trial of poractant alfa (Curosurf) versus beractant (Survanta) in the treatment of respiratory distress syndrome in preterm infants. *Am. J. Perinatol.* 21:109–119.

66. Bernhard, W., J. Mottaghian, A. Gebert, G. A. Rau, H. von der Hardt, and C. F. Poets. 2000. Commercial versus native surfactants. Surface activity, molecular components, and the effect of calcium. *Am. J. Respir. Crit. Care Med.* 162:1524–1533.

67. Parsegian, V. A., R. P. Rand, N. L. Fuller, and D. C. Rau. 1986. Osmotic stress for the direct measurement of intermolecular forces. *Methods Enzymol.* 127:400–416.

68. Parsegian, V. A., R. P. Rand, and D. C. Rau. 2000. Osmotic stress, crowding, preferential hydration, and binding: a comparison of perspectives. *Proc. Natl. Acad. Sci. USA.* 97:3987–3992.

69. Parsegian, V. A., R. P. Rand, and N. L. Fuller. 1991. Direct osmotic stress measurements of hydration and the electrostatic double layer forces between bilayers of double-chained ammonium acetate surfactants. *J. Phys. Chem.* 95:4777–4782.

70. Bligh, E., and W. Dyer. 1959. A rapid method of total lipid extraction and purification. *Can. J. Biochem. Physiol.* 37:911–917.

71. Putz, G., J. Goerke, H. W. Taeusch, and J. A. Clements. 1994. Comparison of captive and modified pulsating bubble surfactometers. *J. Appl. Physiol.* 76:1425–1431.

72. Warriner, H. E., S. L. Keller, S. H. J. Idziak, N. L. Slack, P. Davidson, J. A. Zasadzinski, and C. R. Safinya. 1998. The influence of polymer molecular weight in lamellar gels based on PEG lipids. *Biophys. J.* 75:272–293.

73. Kisak, E., B. Coldren, C. Boyer, C. Evans, and J. A. Zasadzinski. 2004. The vesosome—a multicompartment drug delivery vehicle. *Curr. Med. Chem.* 11:1241–1253.

74. Kisak, E., B. Coldren, and J. A. Zasadzinski. 2002. Nano-compartments enclosing vesicles, colloids and macromolecules via interdigitated lipid bilayers. *Langmuir.* 18:284–288.

75. Viswanathan, R., L. L. Madsen, J. A. Zasadzinski, and D. K. Schwartz. 1995. Liquid to hexatic to crystalline order in Langmuir-Blodgett films. *Science.* 269:51–54.

76. Hui, S. W., R. Viswanathan, J. A. Zasadzinski, and J. N. Israelachvili. 1995. The structure and stability of phospholipid bilayers by AFM. *Biophys. J.* 68:171–178.

77. Krishnan, A., J. Sturgeon, C. A. Siedlicki, and E. A. Vogler. 2003. Scaled interfacial activity of proteins at the liquid-vapor interface. *J. Biomed. Mater. Res.* 68A:544–557.

78. Stenger, P. C., and J. A. Zasadzinski. 2007. Enhanced surfactant adsorption via polymer depletion forces: a simple model for reversing surfactant inhibition in acute respiratory distress syndrome. *Biophys. J.* 92:3–9.

79. Asakura, S., and F. Oosawa. 1958. Interactions between particles suspended in solutions of macromolecules. *J. Polym. Sci. [B].* 33:183–192.

80. Israelachvili, J. N. 1992. Intermolecular and Surface Forces, 2nd ed. Academic Press, London.

81. Lee, K. Y. C., A. Gopal, A. Von Nahmen, J. A. Zasadzinski, J. Majewski, G. S. Smith, P. B. Howes, and K. Kjaer. 2002. Influence of palmitic acid and hexadecanol on the phase transition temperature and molecular packing of dipalmitoylphophatidyl-choline monolayers at the air-water interface. *J. Chem. Phys.* 116:774–783.

82. Bringezu, F., J. Q. Ding, G. Brezesinski, A. J. Waring, and J. A. Zasadzinski. 2002. Influence of pulmonary surfactant protein B on model lung surfactant monolayers. *Langmuir.* 18:2319–2325.

83. Helfrich, W. 1973. Elastic properties of lipid bilayers: theory and possible experiments. *Z. Naturfosch.* 28c:693–703.

84. Helfrich, W. 1978. Steric interaction of fluid membranes in multilayer systems. *Z. Naturforschung.* 33A:305–315.

85. Evans, E., and W. Rawicz. 1990. Entropy driven tension and bending elasticity in condensed fluid membranes. *Phys. Rev. Lett.* 64:2094–2097.

86. Rawicz, W., K. C. Olbrich, T. McIntosh, D. Needham, and E. Evans. 2000. Effect of chain length and unsaturation on elasticity of lipid bilayers. *Biophys. J.* 79:328–339.

87. Jung, H.-T., B. Coldren, J. A. Zasadzinski, D. Iampietro, and E. W. Kaler. 2001. Origins of stability of spontaneous vesicles. *Proc. Natl. Acad. Sci. USA.* 98:1353–1357.

88. Jung, H. T., S. Y. Lee, B. Coldren, J. A. Zasadzinski, and E. W. Kaler. 2002. Gaussian curvature and the equilibrium between cylinders, discs and spheres. *Proc. Natl. Acad. Sci. USA.* 99:15318–15322.

89. Harris, J. 1992. Introduction to biotechnical and biomedical applications of poly(ethylene glycol). *In* Poly(Ethylene Glycol) Chemistry: Biotechnical and Biomedical Applications. J. Harris, editor. Plenum Press, New York. 1–12.

90. Turino, G., and J. Cantor. 2003. Hyaluronan in respiratory injury and repair. *Am. J. Respir. Crit. Care Med.* 167:1169–1175.

91. Sahu, S., A. Tanswell, and W. Lynn. 1980. Isolation and characterization of glycoaminoglycans secreted by human fetal type II pneumocytes in culture. *J. Cell Sci.* 42:183–188.

92. Skinner, S., M. Post, J. Torday, A. Stiles, and B. Smith. 1987. Characterization of proteogylcans synthesized by fetal rat lung type II pneumocytes in vitro and the effects of cortisol. *Exp. Lung Res.* 12:254–264.

93. Bray, B. A. 2001. The role of hyaluronan in the pulmonary alveolus. *J. Theor. Biol.* 210:121–130.

94. Mascarenhas, M. M., R. M. Day, C. D. Ochoa, W. I. Choi, L. Yu, B. Ouyang, H. G. Garg, C. A. Hales, and D. A. Quinn. 2004. Low molecular weight hyaluronan from stretched lung enhances interleukin-8 expression. *Am. J. Respir. Cell Mol. Biol.* 30:51–60.

95. Cantor, J. O., J. M. Cerreta, M. Ochoa, S. Ma, T. Chow, G. Grunig, and G. M. Turino. 2005. Aerosolized hyaluronan limits airspace enlargement in a mouse model of cigarette smoke-induced pulmonary emphysema. *Exp. Lung. Res.* 31:417–430.

96. Cantor, J., B. Shteyngart, J. Cerreta, M. Liu, G. Armand, and G. Turino. 2000. The effect of hyaluronan on elastic fiber injury in vitro and elastase-induced airspace enlargement in vivo. *Proc. Soc. Exp. Biol. Med.* 225:65–71.

97. Forteza, R., T. Lieb, T. Aoki, R. Savani, G. Conner, and M. Salathe. 2001. Hyaluronan serves a novel role in airway mucosal host defense. *FASEB J.* 21:79–86.

98. Nitzan, D. W., U. Nitzan, P. Dan, and S. Yedgar. 2001. The role of hyaluronic acid in protecting surface-active phospholipids from lysis by exogenous phospholipase A(2). *Rheumatology (Oxford).* 40:336–340.

99. Kaplan, P. D., J. L. Rourke, A. G. Yodh, and D. J. Pine. 1994. Entropically driven surface phase separation in binary colloidal mixtures. *Phys. Rev. Lett.* 72:582–585.

100. Zimmerman, S. B., and A. P. Minton. 1993. Macromolecular crowding: biochemical, biophysical, and physiological consequences. *Annu. Rev. Biophys. Biomol. Struct.* 22:27–65.

101. Kaplan, P. D., L. P. Faucheux, and A. J. Libchaber. 1994. Direct observation of the entropic potential in a binary suspension. *Phys. Rev. Lett.* 73:2793–2796.

102. Dinsmore, A. D., D. T. Wong, P. Nelson, and A. G. Yodh. 1998. Hard spheres in vesicles: curvature-induced forces and particle induced curvature. *Phys. Rev. Lett.* 80:409–412.

103. Dinsmore, A. D., A. G. Yodh, and D. J. Pine. 1996. Entropic control of particle motion using passive surface microstructures. *Nature.* 383:239–242.

104. Postle, A. D., E. L. Heeley, and D. C. Wilton. 2001. A comparison of the molecular species compositions of mammalian lung surfactant phospholipids. *Comp. Biochem. Phys. A.* 129:65–73.

105. Robertson, B., and H. L. Halliday. 1998. Principles of surfactant replacement. *Biochim. Biophys. Acta.* 1408:346–361.